Available online at www.sciencedirect.com
SCIENCE DIRECT®
Scripta Materialia 50 (2004) 1283–1288
Scripta MATERIALIA
www.actamat-journals.com

Incidence of atom shuffling on the shear and decohesion behavior of a symmetric tilt grain boundary in copper

F. Sansoz, J.F. Molinari *

Department of Mechanical Engineering, Johns Hopkins University, 104 Latrobe Hall, 3400 North Charles Street, Baltimore, MD 21218, USA

Received 9 December 2003; received in revised form 12 February 2004; accepted 18 February 2004

Abstract

The constitutive response of a Σ9(221) symmetric tilt grain boundary in copper is investigated with an atomistic quasicontinuum method under tension and shear. The maximum strength is found to change with the deformation mode triggered at the interface. Atom shuffling processes cause a major decrease in the intrinsic boundary strength under shear.

Keywords: Grain boundary structure; Grain boundary cohesion; Yield phenomena; Simulation; Quasicontinuum method

1. Introduction

Grain boundary (GB) sliding can be viewed as one of the most fundamental modes of deformation in nanocrystalline (nc) materials at room temperature [1–3]. As the grain size approaches 10–15 nm, the deformation process is no longer dominated by intragranular dislocation activity, but by atom shuffling localized at high-angle grain boundaries [3,4], i.e. a process in which an atom transfers directly from one grain to another without the creation of point defects. Van Swygenhoven and Derlet [4] have studied the mechanism of GB shuffling in nc-FCC metals using molecular dynamics (MD) simulations. These authors have shown that a homogeneous shear stress applied across nc-GB leads to local heterogeneous stress fields that makes a certain number of GB atoms reach the conditions necessary to pass their saddle-point configuration and migrate to a new location. Consequently, the combination of individual atom events makes possible homogeneous sliding of one grain with respect to the other. We aim to provide further insight into the constitutive behavior of nanocrystalline GBs so that relevant information emanating from microscopic shuffling processes is accounted for. A factor impacting on GB shuffling processes is the ability for the crystal lattice to accommodate easily the deformation. In studying slip processes in single crystals, for instance, different authors [5,6] have predicted that unrelaxed crystal assessments lead to systematic overestimates of the misfit energy for slip. Contrarily, in previous atomistic studies on the sliding and decohesion resistance of bicrystals, the lattice has been considered either rigid [7–10] or with an entire freedom to deform [11], but correlations between lattice freedom and GB shuffling events have yet to be addressed. This task is made complicated because deformation processes in bicrystals account for both interface behavior (atom shuffling, sliding, GB dislocations) and grain bulk behavior (lattice dislocations). In the present work, a molecular static method is used to calculate the zero temperature equilibrium structure of a Σ9(221) symmetric tilt grain boundary (STGB) in copper as well as the stress–displacement relationships associated with separation and shear of this bicrystal. The computational procedure is provided in Section 2. In Section 3, quantitative correlations between crystal lattice freedom, atom shuffling and constitutive behavior are presented on the basis of single crystal and Σ9(221) bicrystal simulations.

2. Computational methods

The quasicontinuum (QC) method developed by Tadmor and coworkers [12,13] is used here to simulate cells containing a bicrystal with a GB at its center. A

* Corresponding author. Tel.: +1-410-516-2864; fax: +1-410-516-7254.
E-mail address: molinari@jhu.edu (J.F. Molinari).

1359-6462/$ - see front matter © 2004 Acta Materialia Inc. Published by Elsevier Ltd. All rights reserved.
doi:10.1016/j.scriptamat.2004.02.031

similar approach mixing finite element and atomistic methods was first used on single crystals by Mullins [14]. A partial view of the QC mesh for single crystal is given in Fig. 1a. The QC method proceeds through molecular static energy minimization over an atomistic (non-local) domain and a finite element (local) domain. The constitutive law in these two domains is chosen as the embedded atom (EAM) potential for copper [15], which results in equilibrium lattice constant of 3.615 Å and cutoff distance of 4.950 Å at 0 K. The current method is quasi-planar considering one repeated coincident site lattice (CSL) cell in the out-of-plane direction, i.e. the direction perpendicular to both GB normal and shear direction. The non-local domain is enforced across the entire GB length and within a distance from the GB plane equal to 5.25 times the potential cutoff distance. All simulations are performed with less than 5000 nodes. More details on the QC implementation can be found elsewhere [12,13].

Two separate sets of simulations are used to calculate the GB structure at 0 K equilibrium and the stress–displacement relationships of this structure under tension and shear. The first set to obtain GB equilibrium uses zero force lattice statics technique [16]. The crystals are initially constructed based on the CSL model and defined using the Bravais lattice cell. Different initial configurations are generated by shifting one grain relative to the other, provided that one of the configurations leads to the lowest state in energy after atomic relaxation. The shift vector is defined by the displacement-shift-complete (DSC) lattice. During the relaxation, the total energy is minimized until the addition of out-of-balance forces over the entire system is found less than 10^{-3} eV/Å. The energy minimization process is conducted by a conjugate gradient method. All atoms are free of constraints except for the bottom line of nodes in order to avoid crystal rotation. The GB energy is calculated by subtracting the single crystal energy from the bicrystal energy and dividing by the GB area. To limit surface effects in the energy calculation, only 80% of the bicrystal is considered, therefore excluding atoms near free surfaces.

In the second set, tension and shear simulations are carried out on the 0 K equilibrium structure as described above. Energy minimization is enforced between each loading step. The dimensions of the mesh are kept equal to 184 Å×65 Å for tension and 383 Å×65 Å for shear. We maintain the mesh aspect ratio under shear close to 6 in order to avoid discrepancies related to free surface effects [17]. Previous MD results [18] show that either free or periodic boundary conditions play an important role on the calculated strength of Cu single crystals. In the present case, periodic boundary conditions are not applicable due to the implicit scheme employed in the QC method. Under shear, free boundaries are imposed on left and right columns of atoms, referred to as side atoms in the following. Under tension, the side atoms are fixed in the direction parallel to the GB. These assumptions coupled with the 2D nature of the modeling provide relatively good agreement with 3D MD simulations applying periodic boundaries, as shown below. The present simulations are conducted under

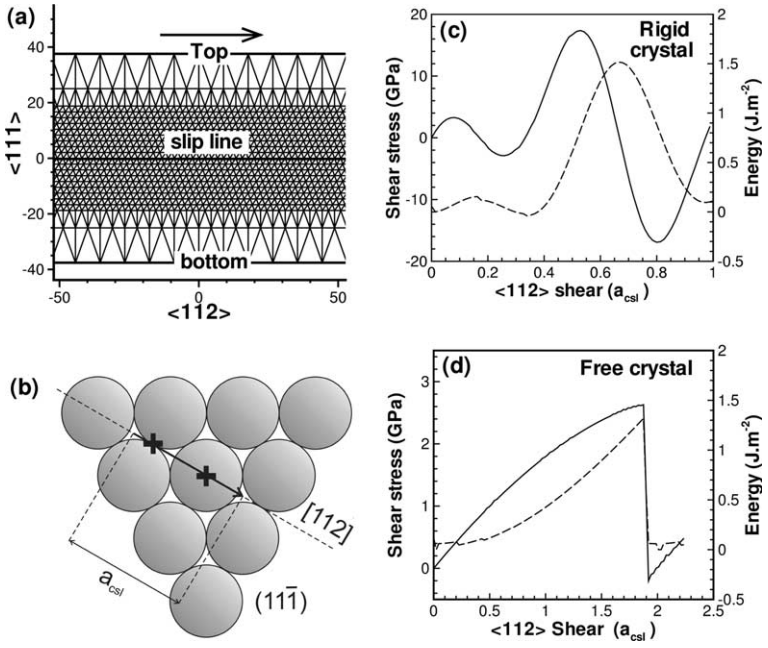

Fig. 1. (a) Quasicontinuum mesh (partial view in Å) used to obtain the energy for $\{1\,1\,1\}\langle 1\,1\,2\rangle$ slip in Cu single crystal under shear. (b) $(1\,1\,\bar{1})$ plane modeled with [1 1 2] shear direction. Shear stress (solid line) and slip energy (dashed line) are shown when the top block of atoms is (c) rigidly or (d) freely shifted with respect to the bottom block of atoms by one $\langle 1\,1\,2\rangle$ Bravais lattice cell. Cross marks in (b) coincide with energy peaks in (c).

displacement-controlled conditions. The mesh is divided into three regions: a fixed block of atoms at the mesh bottom; see Fig. 1a, a region centered on the GB plane where atoms are free of constraints, and a constrained block of atoms located at the mesh top. The number of free atomic planes parallel to the GB and referred to as the extent of crystal lattice freedom in the following, is varied from 0 up to 107. The displacement is applied either parallel or perpendicular to the GB plane to simulate simple shear and tension loading, respectively. All atoms are fixed in the out-of-plane direction. Under shear, when one grain is shifted in shear with respect to the other, a degree of freedom in the direction normal to the GB plane is left to the top block of atoms in order to relax the boundary. The mean stresses in tension and shear are calculated as the addition of projected out-of-balance forces on top constrained atoms and, subsequently, rationalized by the GB area. Finally, in order to visualize planar faults in the FCC crystal during deformation, the central symmetry parameter [19,20] was used with a threshold set to 0.01 so that atoms appear in dark color with perfect FCC stacking and in bright color with planar faults. General software for atomistic visualization [20] was employed for these examinations.

3. Results and discussion

3.1. Single crystal energetics and behavior

The energetics and constitutive behavior of Cu single crystals are examined under tension and shear with different crystal orientations. Homogeneous shear is performed by straining a crystal in a series of incremental shears in a $\langle 1\,1\,2\rangle$ direction on $\{1\,1\,1\}$ planes, referred to as $\{1\,1\,1\}\langle 1\,1\,2\rangle$ shear in the following. The related crystal orientations are given in Fig. 1a. Two types of boundary condition, for which the crystal lattice is kept either perfectly rigid or, conversely, free during deformation, are studied. In a rigid crystal sheared on [1 1 2] direction over a distance of a_{CSL}, as illustrated in Fig. 1b, the energy functional reaches two energy peaks relative to unstable stacking configurations. In this case, the energy and shear stress of the rigid crystal are shown in Fig. 1c. The strength is calculated as the maximum stress causing irreversible behavior, which in this figure is the stress value at the first peak, 3.27 GPa. Fig. 1d shows that the apparent behavior is strongly changed when the crystal lattice deforms freely, and somewhat reminiscent to a stick–slip process, i.e. a non-linear loading followed by a rapid drop after reaching the maximum stress.

The maximum stresses in rigid and free configurations are compared in Table 1. Consistent to earlier works [5,6], this table shows that crystal relaxation causes the significant decrease in maximum stress. In the rigid configuration, some differences can be found as compared to literature results [6,17,18], which may be related to the use of different bonding potentials. On the other hand, the agreement is good in the case of free configurations. The maximum strength for the relaxed copper crystal in $\{1\,1\,1\}\langle 1\,1\,2\rangle$ shear is found equal to 2.45 GPa. This value is within the error obtained from DFT pseudo-potential calculations [6]. For a free copper crystal, applying a displacement perpendicular to the $\{0\,1\,1\}$ planes, referred to as $\{0\,1\,1\}$ tension in Table 1, leads to a maximum tensile strength of 14.97 GPa, which is close to that obtained from EMT potential [18]. Tension curves are not represented for brevity. It is however worth mentioning that a universal binding energy relation (Rose et al. [7]) is only observed in rigid crystals. A different EAM potential (pure Ni [15]) is also tested. As compared to the MD results of Horstemeyer et al. [17] on Ni crystal under $\{0\,1\,1\}\langle 0\,0\,1\rangle$ shear loading, the QC overestimate is less than 8%, which indicates good correlation of QC results with MD.

Finally, we studied the shear of a crystal orientation coinciding with the orientation of one grain in the $\Sigma 9(221)$ STGB tested below. The shear plane on the corresponding crystal orientation is [2 2 1] and the shear direction is $[1\,1\,\bar{4}]$ as shown in Fig. 2a. When applying a shear displacement on a $\{2\,2\,1\}$ plane, the maximum shear stress of a free crystal is found equal to 4.04 GPa (see Table 1). This result will serve hereafter to comment on the role of GB structure relative to the shear strength.

Table 1
Calculated and reference values of strength in Cu and Ni single crystals under different orientations and loading modes

Material	Loading	Maximum stress (rigid crystal)		Maximum stress (free crystal)	
		Calculated	Reference	Calculated	Reference
Cu	$\{1\,1\,1\}\langle 1\,1\,2\rangle$ shear	3.27	4.0 ± 0.1[a]	2.45	2.65 ± 0.2[a]
Cu	{011} tension	20.94	–	14.97	14.3[b]
Ni	$\{011\}\langle 0\,0\,1\rangle$ shear	26.87	–	10.97	10.1[c]
Cu	$\{221\}\langle 1\,1\,4\rangle$ shear	8.54	–	4.04	–

All units of stress in GPa.
[a] Ref. [6].
[b] Ref. [18].
[c] 300 K, Ref. [17].

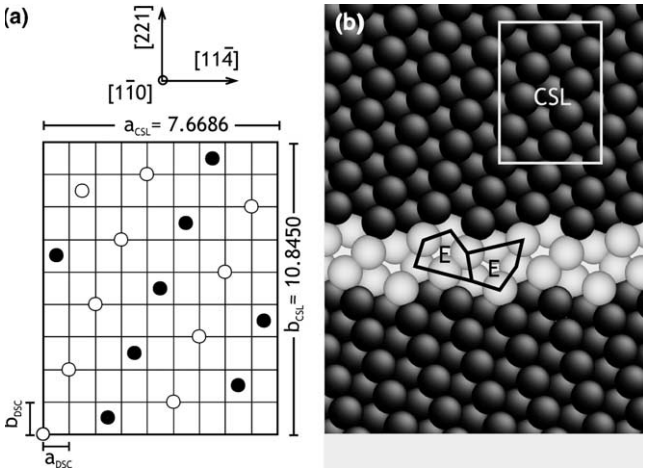

Fig. 2. (a) Σ9(221) coincidence site lattice cell. Open and solid circles indicate different planes of the structure in the ⟨1 1 0⟩ direction. (b) 0 K equilibrium structure for copper Σ9(221) STGB.

3.2. Σ9(221) STGB energetics and behavior

Thirty six initial configurations obtained by shifting the upper grain relative to the lower grain by 9 DSCs in the *x*-direction and 4 DSCs in the *y*-direction were simulated to identify the 0 K equilibrium structure of Σ9(221) STGB. The related CSL model is presented in Fig. 2a along with the DSC vector in both directions. The boundary with the lowest state in energy after lattice relaxation is represented in Fig. 2b. Its periodic structure is compliant with two E structural units as predicted from MD calculations in low stacking fault energy FCC metals [16]. The 0 K equilibrium energy is found equal to 831 mJ/m^2 for the shear model and 833 mJ/m^2 for the tension model, while the value predicted from MD is equal to 771 mJ/m^2 [21]. The differences may be interpreted by the lack of periodic boundaries in QC: the smaller the GB area, the more significant the boundary effects and the higher the GB energy.

The shear and tensile stresses of Σ9(221) STGB undergoing shear and normal applied displacements, respectively, are given in Fig. 3 as a function of the extent of crystal lattice freedom maintained during loading. For all loading conditions, a maximum stress is reached when a displacement less than few angstroms is applied. The critical displacement Δ_c associated with the maximum stress is found to increase with crystal lattice freedom. This is explained through the elastic contribution of the lattice, resulting in the apparent loss of the bicrystal modulus and, conversely, increasing Δ_c. The ratio of bicrystal modulus over single crystal modulus in free configurations is found equal to 0.87 and 0.94, in shear and tension, respectively. This suggests that for systems of sizes around 6.5 nm, the elastic moduli of the GB region are not strongly different from that of the crystal. In contrast, the maximum shear stress in Σ9(221) STGB is reduced from 19.5 GPa to only 3.5 GPa with seven free atomic planes, while the tensile stress is reduced from 16.7 to 15.4 GPa for the same number of planes as shown in Figs. 3a and b. Therefore, the extent of crystal lattice freedom has a strong effect on the shear stress.

Hereafter, our intent is to gain fundamental understanding of the strength differences between tension and shear and to correlate the values of maximum stress to the nature of GB deformation processes. The maximum stress for shear is represented in Fig. 3c as a function of free atomic planes in the GB vicinity. In this figure, three plateaus of maximum stress can be identified, being equal to 5.3, 3.4 and 1.6 GPa, and denoted stages I, II and III, respectively. The deformation mechanism for each of these stages is depicted in Fig. 4a. In stage I, the GB is cleaved and the crystal lattice remains quasi-rigid. During stage II, stick–slip events occur similarly to what was observed in the free single crystal and uncorrelated atom shuffling is observed at the boundary. The magnitude of individual atomic events tends to increase as the extent of crystal lattice freedom increases. No lattice

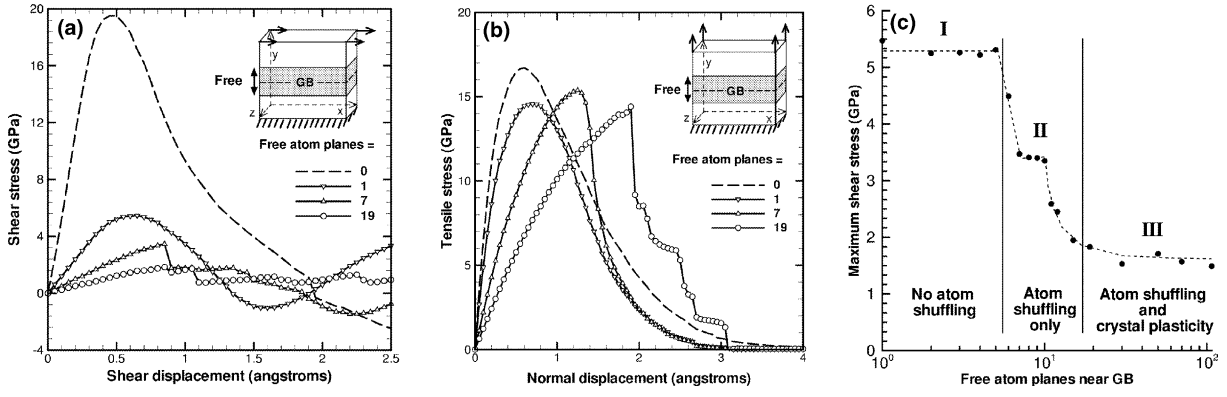

Fig. 3. Influence of GB atomic freedom on the constitutive behavior of copper Σ9(221) STGB: (a) shear loading, (b) tensile loading, (c) maximum shear stress versus number of free atom planes near GB.

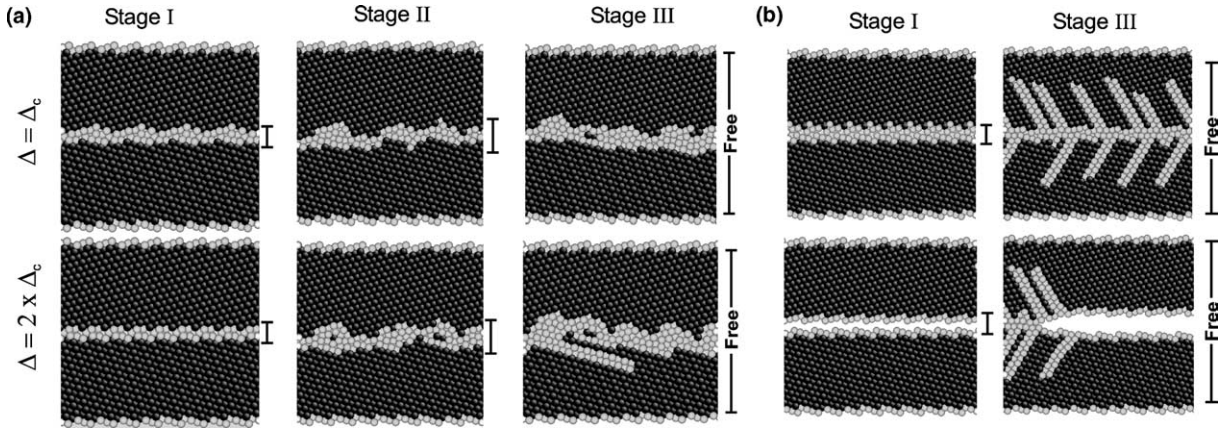

Fig. 4. GB deformation mechanisms associated with the three plateaus of maximum stress in Fig. 3c for (a) shear and (b) tension. Atoms in dark color have perfect FCC crystal stacking, while atoms in bright color are GB regions, planar faults and partial dislocations. Δ_c represents critical displacement at maximum stress. The extent of crystal lattice freedom is also indicated.

dislocations, however, are observed in this mode. Stage III, which only operates with relatively large extents of crystal freedom as shown in Fig. 4a, results from the interplay between GB atom shuffling and bulk crystal plasticity. Crystal plasticity is evidenced in the form of partial dislocations emanating from sites where atomic shuffling is important. In tension, however, our results provide no evidence of intermediate stage II plateau; the level of stress varying progressively from stages I to III. The decrease of maximum tensile stress is linked to the creation of GB partial dislocations only since atom shuffling is absent in tension, as shown in Fig. 4b. When stage III is reached, the tension model predicts progressive separation of the GB from one side to the other. In conclusion, it may be thought that, in tension, GB act as partial dislocation sources accelerating crystal damage and GB-related atom shuffling has limited role in this mode, while, in shear, it is the predominant factor responsible for the decrease of boundary strength and the presence of a stage II plateau in maximum shear stress. This is supported by the fact that the maximum shear stress is significantly less in Σ9(221) STGB than in a single crystal tested with same orientation, for which no shuffling prevails. This value is equal to 1.53 and 4.04 GPa, respectively, when the cell is entirely free.

The above analysis is used to draw a general assessment in the determination of constitutive behavior with regard to nc boundaries. An important factor is the ability to model separately intrinsic GB relations; i.e. bonding and atom shuffling, and crystal plasticity effects; i.e. partial dislocations emanating from GB free volume in the current study. As such, it is suggested with the current GB structure, that maintaining seven atomic planes free to deform is necessary to achieve stage II, where intrinsic GB events occur, but it is required not to exceed 12 atomic planes in order to avoid bulk effects. Keeping this rule in mind, we determine the maximum strength of Σ9(221) STGB at 0 K to be equal to the plateau in stage II, 3.47 GPa in shear and to that in stage I, 15.39 GPa, in tension. In the regime where GB sliding is the predominant mode of deformation, previous MD studies [22] have determined that the flow stress of nc-copper is 1.19 GPa higher at 0 K than 300 K, independently of grain size considerations. Accordingly, the maximum shear strength predicted here at 0 K can be corrected to 2.28 GPa at 300 K. This value is in surprisingly good agreement with the maximum strength for nc-copper of 2.25 GPa determined by MD [3]. While Σ9(221) STGB is reported experimentally to have lower sliding stress at low temperature than other ⟨0 1 1⟩ STGB bicrystals [23], it should be noted that symmetric GB structure may be relatively sparse in nc metals. Indeed, it has been observed in conventional polycrystalline copper, that asymmetric tilt grain boundaries (ATGB) are most predominant [24]. Having higher equilibrium energy than STGB, ATGB are likely to possess lower shear strength either. Further simulations are currently underway to determine the significance of GB nature on constitutive behavior.

4. Concluding remarks

In conclusion, the QC method is shown to provide useful insights in determining the local constitutive response of nc metals from atomistic. The maximum strength for GB is highly dependent upon the extent of crystal lattice freedom and the nature of deformation processes in GB vicinity. Under shear, there exists a fundamental limit in this extent in order to capture uncorrelated atom shuffling events without crystal plasticity effects. This limit is based upon the presence of a plateau in maximum shear stress detected when atom shuffling is triggered. The simulations show that Σ9(221)

STGB is about 4.5 times weaker in shear than in tension. The maximum shear strength for this bicrystal is found to be very close to that of nc-copper [3].

Acknowledgements

This work was performed under the auspices of NSF-Nanoscale Interdisciplinary Research Team under contract DMR-0210215 and ARL-Center for Advanced Materials and Ceramic Systems under the ARMAC-RTP Cooperative Agreement Number DAAD19-01-2-0003. We are grateful to the developers of the QC method for providing their code [25] and to K.J. Hemker for helpful comments.

References

[1] Weertman JR, Farkas D, Hemker K, Kung H, Mayo M, Mitra R, et al. MRS Bull 1999:44.
[2] Van Swygenhoven H, Weertman JR. Scripta Mater 2003;49:625.
[3] Schiotz J, Jacobsen KW. Science 2003;301:1357.
[4] Van Swygenhoven H, Derlet PM. Phys Rev B 2001;64:224105.
[5] Miller R, Phillips R. Philos Mag A 1996;73:803.
[6] Roundy D, Krenn CR, Cohen ML, Morris Jr JW. Phys Rev Lett 1999;82:2713.
[7] Rose JH, Ferrante J, Smith JR. Phys Rev Lett 1981;47:675.
[8] Chandra N, Dang P. J Mater Sci 1999;34:655.
[9] Namilae S, Chandra N, Nieh TG. Scripta Mater 2002;46:49.
[10] Grujicic M, Cao G, Joseph PF. Int J Multiscale Comp Eng 2003;1:1.
[11] Kurtz RJ, Hoagland RG. Scripta Mater 1998;39:653.
[12] Tadmor EB, Ortiz M, Phillips R. Philos Mag A 1996;73:1529.
[13] Shenoy VB, Miller R, Tadmor EB, Rodney D, Phillips R, Ortiz M. J Mech Phys Solids 1999;47:611.
[14] Mullins M. Scripta Metall 1982;16:663.
[15] Foiles SM, Baskes MI, Daw MS. Phys Rev B 1986;33:7983.
[16] Rittner JD, Seidman DN. Phys Rev B 1996;54:6999.
[17] Horstemeyer MF, Baskes MI, Prantil VC, Philliber J, Vonderheide S. Model Simulat Mater Sci Eng 2003;11:265.
[18] Heino P, Hakkinen H, Kaski K. Euro Lett 1998;41:273.
[19] Kelchner CL, Plimpton SJ, Hamilton JC. Phys Rev B 1998;58:11085.
[20] Li J. Model Simulat Mater Sci Eng 2003;11:173.
[21] Wolf D. Acta Metall Mater 1990;38:781.
[22] Schiotz J, Vegge T, Di Tolla FD, Jacobsen KW. Phys Rev B 1999;60:11971.
[23] Monzen R, Kuze T, Matsuda O, Miura H. Met Mater Trans A 2003;34A:773.
[24] Randle V. Acta Mater 1997;46:1459.
[25] The QC method home page. Available from <www.qcmethod.com>.